

The Laser Microchemical Lathe: Rapid Freeform Part Fabrication from the Vapor Phase

K. Williams, N. Jaikumar, G. Saiprasanna, M. Hegler, J. Maxwell*

Institute for Micromanufacturing, Louisiana Tech Univ., 911 Hergot Ave., Ruston, LA, USA

This paper reports the development of a two-beam Laser Microchemical Lathe (LML) used for prototyping freeform axi-symmetric parts from the vapor phase. In the LML, one beam is focused along the rotational axis of the lathe, while another is scanned at right angles to the first. The first beam is used for alignment and to deposit a fiber-like mandrel from a vapor-phase precursor. The second beam is then applied to add or remove material on this rotating mandrel, either through high pressure laser chemical vapor deposition (LCVD) or laser chemical vapor etching (LCVE). Material is added when an appropriate precursor is present, or removed when a reducing atmosphere such as chlorine, iodine, or hydrogen is employed. In LCVE mode, the second beam may be scanned in profile along the length of a rotating part—thereby profiling the part by laser etching. The ability to correct for errors in the deposition process through such laser profiling allows accurate prototyping of milli-scale axi-symmetric parts, such as lead screws, cams, and sharp needles. Very rapid deposition and etching rates were achieved; at ethylene pressures above 10 atmospheres, diamond-like carbon was grown at linear rates exceeding 120,000 microns per second (12 cm/s). This record-setting growth rate allows the computer-controlled prototyping of carbon-fiber reinforced structures with volumes surpassing 1 cubic centimeter in only 10-20 minutes.

Keywords: High Pressure Laser Chemical Vapor Deposition, Carbon, Alkenes, Direct-writing, Freeform Growth.

I. Introduction

Previous efforts in vapor-phase solid freeform fabrication have concentrated on the growth of transition and refractory metals,¹ implementation of emissions and temperature feedback control methods,^{2,3} exploring self-limiting effects,⁴ and prototyping functional devices such as springs, microsolenoids, and waveguides.^{5,6} The rapid growth of fibers at axial rates approaching 1 mm/s has also been demonstrated at elevated pressures.⁷

While it has been shown that three-dimensional laser chemical vapor deposition (LCVD) may be employed to grow simple freeform parts, the process is inherently unstable when operating in the kinetically-limited regime; this is especially apparent during repetitive laser scanning, where irregularities in one layer are amplified in the next, resulting in very irregular deposits.⁸ It is for this reason that the emissions and temperature feedback control methods mentioned above are being investigated, as well as the use of elevated pressures which facilitate mass-transport limited growth.

An alternate feedback approach also holds promise, where imperfections in the laser deposited surface are corrected through laser ablation or three-dimensional laser chemical vapor etching (3D-LCVE). In this case, a reducing atmosphere is employed, rather than a CVD precursor, and the by-products are volatile. Rapid chlorine etching of silicon and other materials via 3D-LCVE has been demonstrated by various investigators.⁹ Note that it is possible to switch between 3D-LCVD and 3D-LCVE on-the-fly by merely changing chamber gases; this allows material to be added to (or deleted from) any portion of an object, either to correct for machining errors produced during laser deposition or to generate three-dimensional shapes

* Corresponding Author: maxwell@coes.latech.edu

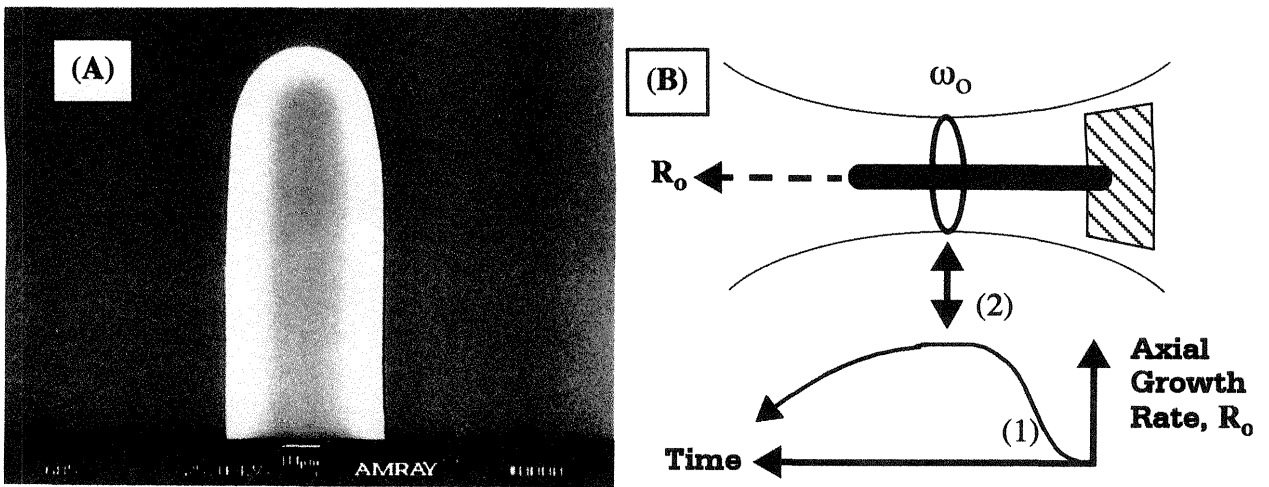


Fig. 1: (A) Carbon Fiber, (B) Rod Growth Rate Measurements

which cannot be fabricated by usual means. The emissions and temperature feedback techniques currently under development will also be essential for this task, allowing precise volumes of material to be deposited or removed in a selected area. The combined 3D-LCVD/E processes may also be used to build up or etch the surfaces of existing objects, creating periodic or arbitrary perturbations over surfaces in a controlled manner.

The objective of this paper is two-fold: first to demonstrate the potential of high pressure, convectively-enhanced, laser chemical vapor deposition (HPCE-LCVD) for high-speed prototyping through fiber growth in excess of 1 mm/s; and second, to implement a new laser prototyping tool, termed the Laser Microchemical Lathe (LML), which may be harnessed to accurately machine small axi-symmetric parts with the combined 3D-LCVD/E processes. To this end, growth rate data for carbon fibers grown from the alkenes, including ethylene, butene, pentene, hexene, and heptene will be presented, as well as preliminary results in part fabrication with the LML.

II. Experimental Method

A) Fiber Growth

For the carbon growth experiments, several hundred fibers were grown from the alkenes. To accurately measure the steady-state axial fiber growth rate, the prime focus of the laser beam was fixed 250-300 microns in front of the substrate, as shown in Fig. 1B. In this way, it was possible to eliminate focal offset errors which may occur during laser tracking, and ensure that the fibers had passed out of the transient growth regime (1), where conduction to the substrate influences the growth rate. A minimum of 12 axial rate measurements were then performed along the length of each rod, to decouple the effects of varying beam waist on the axial rate. The maximum measured rate corresponded to the position of the optimal focus—point (2) in Fig. 1B. A full description of rod growth throughout the transient, steady-state, and tail regimes has been previously provided.¹⁰

For the fiber growth experiments, a small chamber was employed with double windows at each port. The space between each window-assembly was heated continuously with a flow of hot air to eliminate precursor condensation on the inside window. The entire chamber and gas delivery system were also heated to a temperature greater than that of the precursor source cyl-

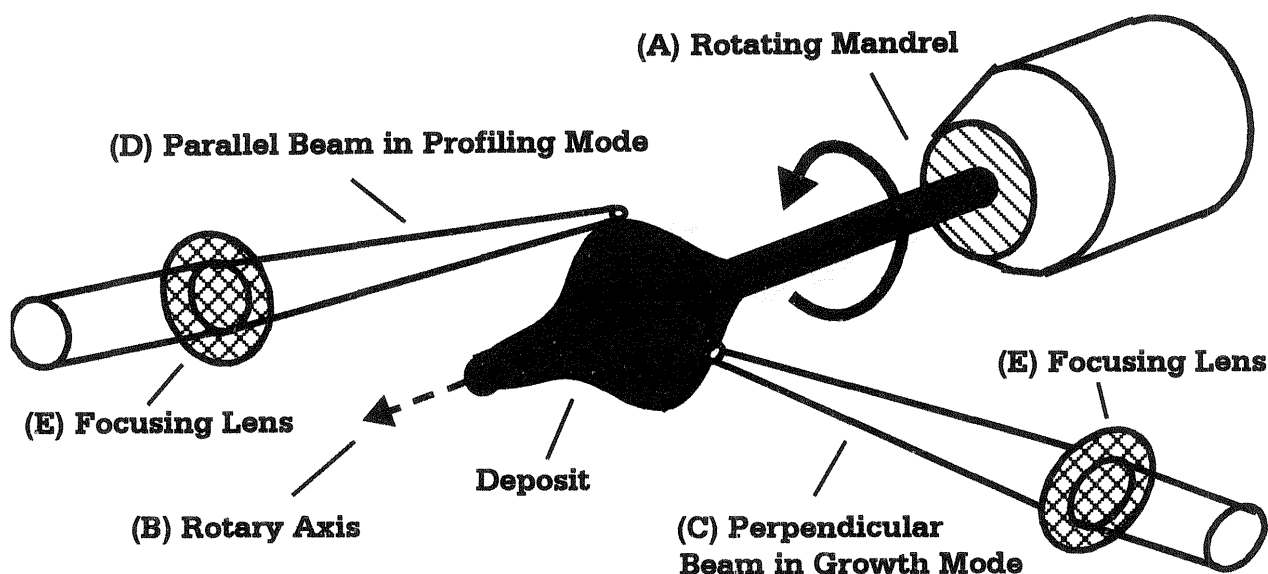


Fig. 2: Principle of the Laser Microchemical Lathe

inder. Two gas regulators were attached at the inlet and outlet of the chamber, so that a high pressure flow of gas could be maintained through the chamber, while the chamber pressure remained constant. At the inlet, this precursor gas stream was directed toward the substrate through a 2 mm ID nozzle, allowing forced convection over the reaction zone. This nozzle could be oriented in a variety of configurations (parallel, perpendicular, or behind the substrate). In this case, a 40 W Nd:YAG laser beam was focused to a 20-25 μm spot using a laser best-form lens. Tungsten light bulb filaments 40 μm in diameter were used as substrates.

B) The LML: Principle and Design

To implement the Laser Microchemical Lathe (LML), an initial fiber (the substrate) was grown on a rotating mandrel—as shown in Fig. 2 (A), so that the substrate was auto-aligned to the rotary axis (B). Two beams were then focused at right angles onto this substrate, one perpendicular to the rotary axis (C), and the other parallel to the axis (D). Depending on the ambient gas present, either beam could be used for 3D-LCVD or 3D-LCVE. In the first case, the beam was focused normal to the deposit surface as in (C)—so that material could be added to the cross section of the part. In the latter case (LCVE), the beam was passed at grazing incidence to the deposit surface, removing excess material which protruded beyond the desired contour—as in Fig. 2 (D). Either beam could be used for profiling or deposition, and the beams could be focused to a common point, or used independently as desired.

A schematic of the entire LML system is shown in Fig. 3. As before, a small chamber with heated windows (a) was employed with a heated gas delivery system and a nozzle (b) directed at the substrate. In this case, however, a mandrel (such as that in Fig. 2) was supported by two precision bearings inside the chamber and driven by a rotary feedthrough (c) with stepper-motor actuation. The parallel and perpendicular beams were delivered to the LML through fiber optics (d), plate beamsplitters (e), and objective lenses (f). In both cases, the beamsplitters and lenses rode on 6-axis piezoelectric stages (g), so that each beam could be independently aligned to the deposit. The piezoelectric stages and rotary axis stepper motor were positioned with a high-speed data acquisition system and motion controller. The beamsplitters were designed to reflect the beam efficiently at 1064 nm, while passing higher wavelengths

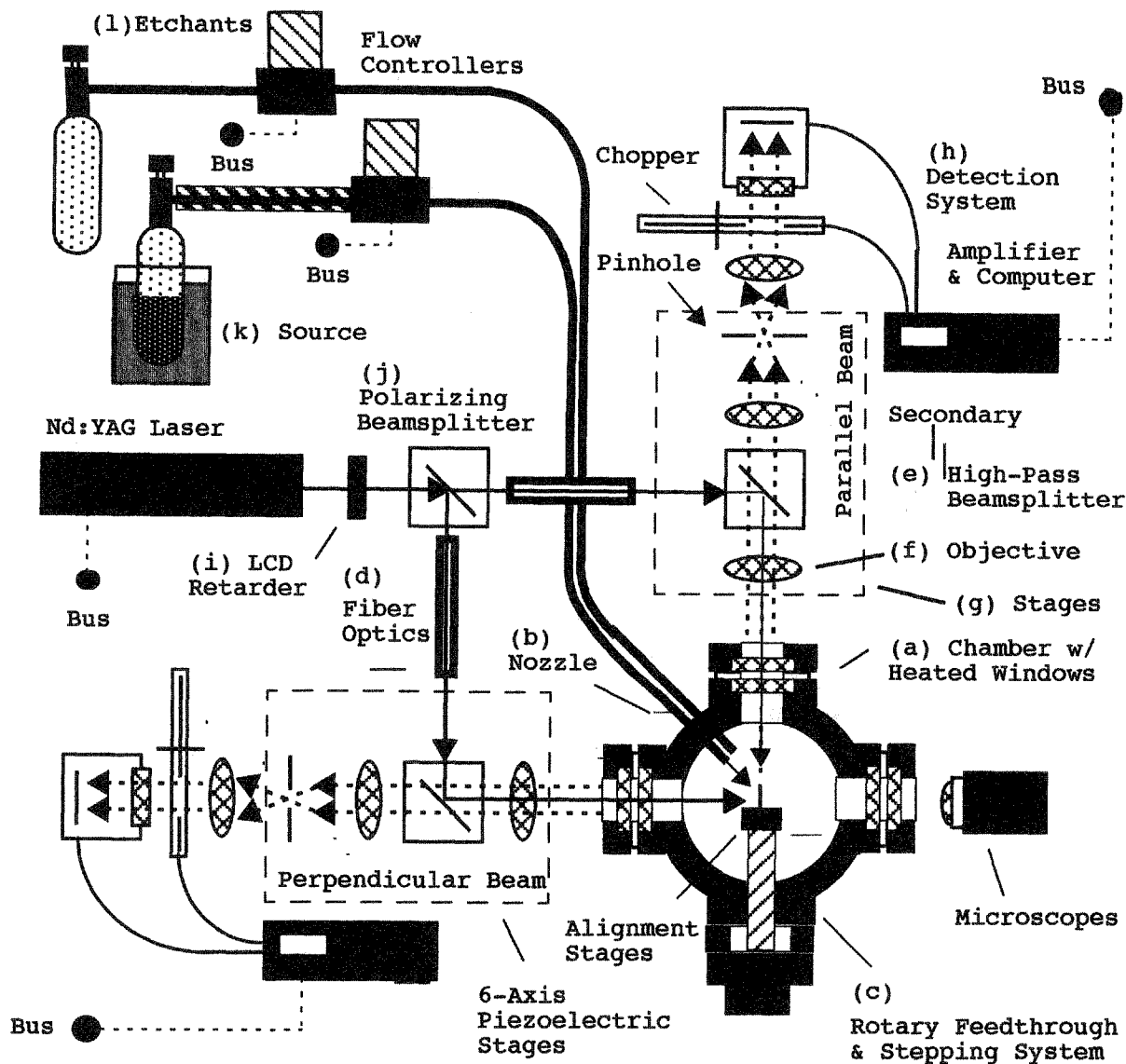


Fig. 3: Experimental Apparatus (Overview)

from 1300 to 1600 nm. In this way, the reaction could be monitored from behind the beam-splitter, with the detection system (h), which has been previously described for temperature and emissions feedback control.¹¹ Finally, to allow for both deposition and profiling, the gas delivery system allowed the introduction of both precursors (k) and etchants (l) into the chamber through the nozzle (b).

For deposition, the Nd:YAG laser was operated in cw mode, while for profiling the laser was Q-switched, with peak powers of up to 60kW. At low powers, the beam was modulated with a liquid crystal retarder (i) through a polarizing beamsplitter (j), with peak-to-peak power swings in under 20 ms. All laser powers reported herein were corrected for optical losses, and represent the actual beam power present at the deposit.

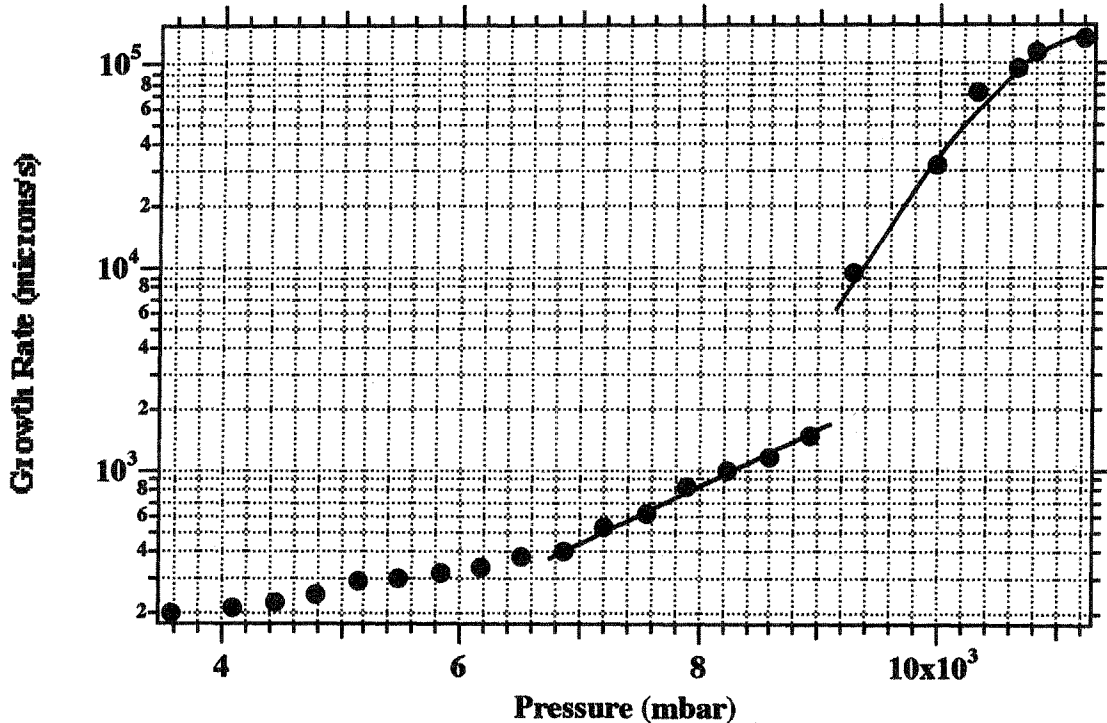


Fig. 4: Fiber Axial Growth Rate vs. Ethylene Pressure at Constant Laser Power (950 mW)

III. Results

A) Carbon Growth Experiments from the Alkenes

While carbon rods have been grown previously from acetylene,¹² methane,¹³ and ethylene,¹⁴ there appears to be no previous data of vapor-phase fiber growth from heavier molecular weight hydrocarbons. For this paper, the ethylene series, including ethylene, butene, pentene, hexene, and heptene was investigated at elevated vapor pressures.

As a baseline for comparison, several hundred fibers were grown from pure ethylene. The axial growth rate of the carbon fibers is shown in Fig. 4 for ethylene pressures from 4-11 bar. In this case, the laser power was held constant at 0.95 W. The most striking feature of this graph is the sudden discontinuity and rapid rise in growth rates above pressures of 9.3 bar; on a linear plot, it appears that the growth rate is directly proportional to the pressure in this regime, with no apparent sign of saturating. At 11 bar, the carbon fibers grew at an impressive 120,000 $\mu\text{m/s}$ (12 cm/s), a record setting growth rate for LCVD. The data points at the highest pressures were repeated several times to confirm these axial rates. One 120 μm diameter fiber grew at over 130,000 $\mu\text{m/s}$, corresponding to a volumetric deposition rate of 1.5 mm^3/s . At this speed, a 1 cm^3 object could be prototyped in 11 minutes—sufficient for large scale rapid prototyping.

Another notable feature of Fig. 4 is the change in growth rate at 6.5 bar. At lower pressures, the growth rate rises linearly from 4 bar to approximately 6.5 bar, then begins an exponential rise which continues until 9.3 bar. As the reaction rate was transport limited at these pressures,

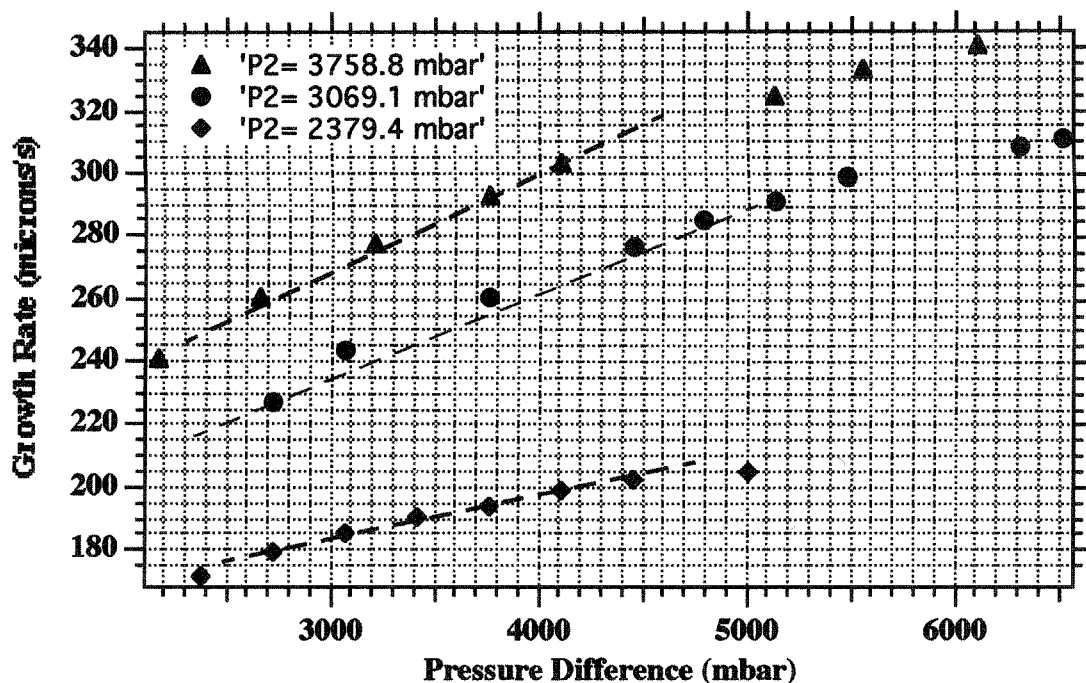


Fig. 5: Axial Growth Rate vs. Mass Flow Rate: Ethylene

it appears that increasing pressure allowed greater transport through enhanced convection and supersaturation of the reaction zone with ethylene molecules.

At 9.3 bar, a corresponding change in rod morphology was also observed; fully-dense diamond-like carbon grew below 9.3 bar, while porous carbon fibers were obtained at higher pressures. However, the porous fibers were still cohesive and highly flexible. The diamond-like carbon fibers exhibited the same highly elastic properties described previously;⁵ they were fully-dense over a wide range of laser powers—allowing the fiber diameter to be tailored to particular applications without a significant change in material properties. At laser powers above approximately 2.5-3.0 W (depending on the pressure) graphite fibers formed which were comparatively brittle. In Fig. 7A, a fiber is shown which passed through the optimal focus as a graphitic deposit, then as the incident laser power density dropped, smooth diamond-like deposits were obtained. At powers above 3.0 W homogeneous nucleation of carbon particles in the gas phase also occurred around the growth zone; these particles could be used to track the fluid flow around the fiber. Very rapid convection was observed, in excess of meter/second velocities near the laser heated zone. At the highest powers, carbon particles accumulated at the upper window of the chamber, directly above the carbon fibers—marking the rapid upward convection of the precursor fluid.

Forced convection experiments were also performed, using the two-regulator system described above. To obtain a variety of mass flow rates, the inlet regulator pressure was varied while maintaining a constant chamber pressure with the outlet regulator. In this case, a 50-200% increase in axial growth rate was observed over static data. The nozzle was directed normal to the fiber axis, and horizontally, i.e. perpendicular to the axis of natural convection. This can be seen in Fig. 5, where the ethylene flow rate is represented by the difference in chamber and inlet-regulator pressures—for three different base pressures. As the pressure difference (flow rate) rose, so did the axial rate—with a slope of approximately 20-30 $\mu\text{m/s}\cdot\text{bar}$. The fibers grew visibly faster as they passed through the forced nozzle flow; while no axial direc-

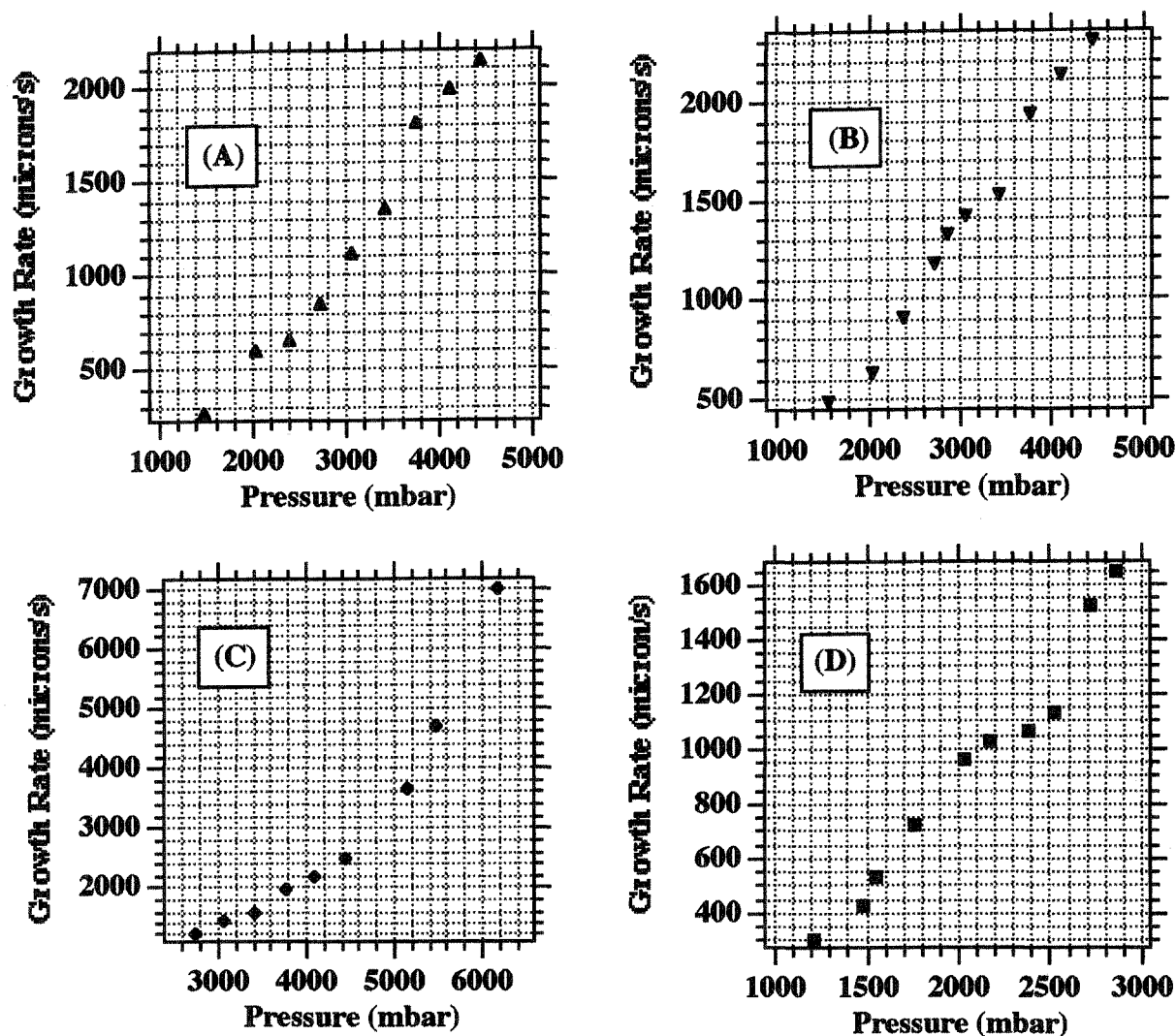


Fig. 6: Growth Rates vs. Pressure:
 (A) Butene, (B) Pentene, (C) Hexene, (D) Heptene

tionality has as yet been observed, the fibers were slightly out-of-round due to the cross-flow. Note that the nozzle diameter of 2 mm was large compared to the growth zone on the fiber. An important feature to note in Fig. 5 is that the rate enhancement tends to saturate at the highest flow velocities; this is tentatively explained by forced cooling of the rods—as the same laser power was used throughout the experiment. It remains to be seen whether it is possible to compensate for the forced cooling with an increase in the incident laser power. However, the potential for more rapid growth through forced convection is apparent.

To investigate the potential of the longer chain hydrocarbons, fibers were also grown from 1-butene (C_4H_8), 1-pentene (C_5H_{10}), 1-hexene (C_6H_{12}), and 1-heptene (C_7H_{14}), respectively. As these precursors are all liquids at room temperature, the heated chamber and gas delivery system were employed. In Fig. 6, the axial growth rate for each these precursors is displayed; while the pressure was varied, a constant laser power of 950 mW was maintained throughout the growth experiments. The slowest axial rates among these precursors were obtained with butene in Fig. 6A. However, a comparison of Fig. 4 (ethylene) and Fig. 6A (butene), reveals

that for equivalent vapor pressures and laser powers, butene provides the greater deposition rate, by nearly an order of magnitude!

A further comparison of Fig. 6B, Fig. 6C, and Fig. 6D shows that for equivalent pressures, the growth rate rises with increasing molecular weight of the precursor, with heptene yielding the highest deposition rates. While not surprising, this result confirms that longer-chain hydrocarbons are desirable for the maximum possible growth rates, despite lower diffusion constants due to increased molecular weight. While each of the alkenes were studied at pressures of up to 3 bar, hexene (C) was investigated at pressures of up to 6.15 bar, yielding smooth fibers at axial rates of 7 mm/s! At an equivalent pressure, ethylene produced fibers at only 320 $\mu\text{m/s}$. Finally, the morphologies of the fibers grown from the longer-chain alkenes were similar to those obtained with ethylene. At laser powers below 2-3 W, diamond-like fibers resulted, while excessive powers yielded graphitic rods.

B) The Laser Microchemical Lathe

The LML was also implemented, as seen in Fig. 7A, using ethylene as a precursor. As expected, the diameter of the carbon mandrel fiber could be broadened through laser deposition, such as in Fig. 2 (C)—and etched as in Fig. 2 (D). Preliminary runs with the system yielded several sample parts, including rings, helices, pinafore spirals, and spur-gear-like parts. In the latter case, the teeth of the gear were laser-ablated to obtain uniform tooth heights, and then filleted between the teeth by laser deposition (see Fig. 7C). Future work will concentrate on implementing feedback control schemes to obtain consistently smooth deposits during repetitive scanning operations, as well as the growth of more complex and useful axi-symmetric parts.

IV. Acknowledgments

The authors would like to thank the National Science Foundation and the Louisiana Board of Regents Research Competitiveness Program for their generous support for this work. We would also like to thank Robert Giasolli and Philip Coane for their contributions in facilities installations and chemical handling and disposal.

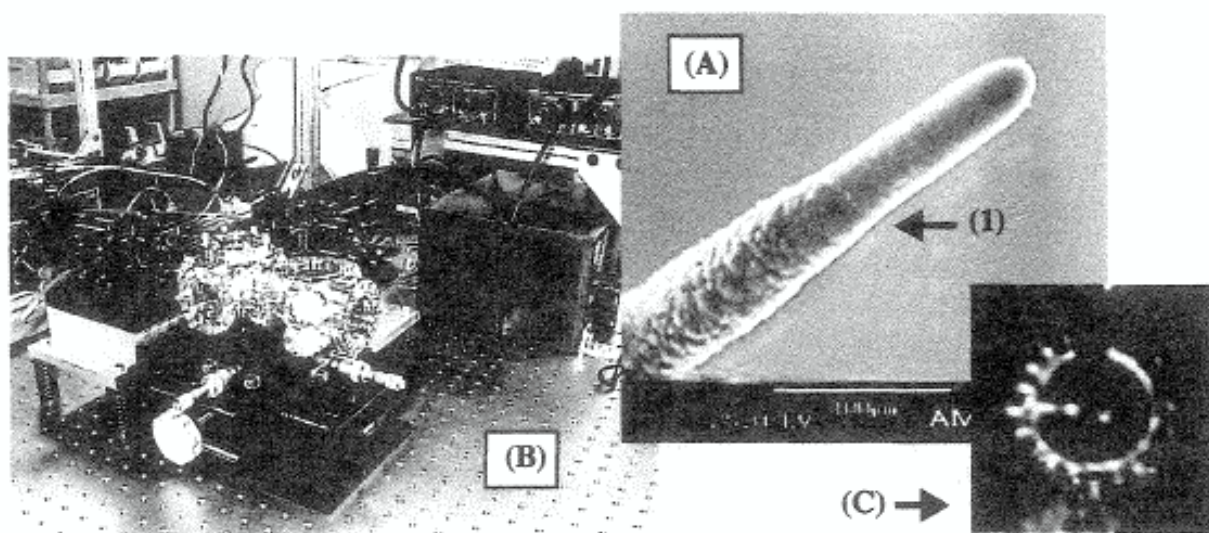


Fig. 7: (A) Transition Between Graphitic and Diamond-like carbon, (B) Carbon The Laser Microchemical Lathe, (C) Gear-like Deposit (video)

V. Bibliography

1. Maxwell, J., Pegna, J., DeAngelis, D., Messia, D., "Three-dimensional Laser Chemical Vapor Deposition of Nickel-Iron Alloys," Material Research Society Symposium Proceedings, v. 397 (B3.30): Advanced Laser Processing, MRS Fall 1995 Meeting, Boston, MA (Nov. 27--Dec.1, 1995).
2. Maxwell, J., Pegna, J., DeAngelis, D., "Feedback Control and Reaction Kinetics of Three-dimensional Laser Chemical Vapor Deposition" Applied Physics A, Vol. 67, (1998), pp. 323-329.
3. Thissell, W., Marcus, H. L., "New Developments in Processing and Control of Selected Area Laser Deposition of Carbon," Proc. Solid Freeform Fabrication Symposium, Austin, Texas, (Aug. 1994), pp. 311-320.
4. Maxwell, J., Krishnan, K., "High-Pressure, Convectively-Enhanced, Laser Chemical Vapor Deposition of Titanium," Proc. Solid Freeform Fabrication Symposium, Austin, Texas, (Aug. 1997).
5. Maxwell, J., Larsson, K., Boman, M., "Rapid Prototyping of Functional Three-Dimensional Microsolenoids and Electromagnets by High-Pressure Laser Chemical Vapor Deposition" Proc. Solid Freeform Fabrication Symposium, Austin, Texas, (Aug. 1998).
6. Wanke, M. C., Lehmann, O., Stuke, M., "Laser Rapid Prototyping of Photonic Band Gap Microstructures," Science, Vol. 275, No. 5304, (Feb. 28 1997), p. 1284.
7. Wallenberger, F. T., Nordine, P. C. "Amorphous Silicon Nitride Fibers Grown from the Vapor Phase," J. Mater. Res., Vol. 9, No. 3, (Mar. 1994), pp. 527-530.
8. Pegna, J., Messia, D., Maxwell, J., DeAngelis, D., "Real-time Control and Modelling for the Laser Chemical Vapor Deposition of Walled-Structures," Material Research Society Symposium: Rapid Prototyping, MRS Spring 1997 Meeting, San Francisco, CA (Apr. 1997).
9. Bloomstein, T. M., Ehrlich, D. J., "Stereo Laser Micromachining of Silicon," Applied Physics Letters, Vol. 61, No. 6, (10 Aug. 1992), pp. 708-710.
10. Maxwell, J., Ph.D. Thesis, Rensselaer Polytechnic Institute, Ch. 5 and 6.
11. Maxwell, J., Williams, K., Larsson, K., Boman, M., "Freeform Fabrication of Functional Microsolenoids, Electromagnets and Helical Springs Using High-Pressure Laser Chemical Vapor Deposition," IEEE Micro Electro Mechanical Systems (MEMS) Conference, Orlando, FL, Jan. 1999.
12. Zong, G., Tompkins, J., Thissell, W., Sajot, E., Marcus, H., "Processing Problems Associated with Gas Phase Solid Freeform Fabrication Using Pyrolytic Selective Area Laser Deposition," Proc. Solid Freeform Fabrication Symposium, (1991), pp. 271-278.
13. Wallenberger, F. T., Nordine, P., "Strong, Pure, and Uniform Carbon Fibers Obtained Directly from the Vapor Phase," Science, Vol. 260, (1993), pp. 66-68.
14. Maxwell, J., Pegna, J., "Laser-induced Pyrolysis of Tapered Microstructures," Proc. Solid Freeform Fabrication Symposium, Austin, Texas, (Aug. 1995).

